CIP4 Targeted to Recruit GTP-Cdc42 Involving in Invadopodia Formation Through NF-κB Signaling Pathway Promotes Invasion and Metastasis of Colorectal Cancer

Zhiyan Hu
Southern Medical University School of Basic Medical Sciences
Jiaxian Zhu
Shenzhen Hospital of Southern Medical University
Yidan Ma
Southern Medical University
Ting Long
Shenzhen Hospital of Southern Medical University
Lingfang Gao
Shenzhen Hospital of Southern Medical University
Yan Zhong
Shenzhen Hospital of Southern Medical University
Xiaoyan Wang
Southern Medical University School of Basic Medical Sciences
Zuguo Li (Lizg@smu.edu.cn)
ShenZhen Hospital of Southern Medical University

Research

Keywords: CIP4, Cdc42, NF-κB, invadopodia, colorectal cancer, invasion and metastasis

Posted Date: May 7th, 2021

DOI: https://doi.org/10.21203/rs.3.rs-433625/v1

Abstract

Background

CIP4 (Cdc42-interacting protein 4), a member of the F-BAR family which plays an important role in regulating cell membrane and actin, has been reported to interact with Cdc42 and closely associated with tumor invadopodia formation. However, the specific mechanism of the interaction between CIP4 and Cdc42 as well as the downstream signaling pathway in response in colorectal cancer (CRC) remains unknown, which is worth exploring for its impact on tumor infiltration and metastasis.

Methods

Immunohistochemistry and western blot analyses were performed to detect the expression of CIP4 and Cdc42. Their relationship with CRC clinicopathological characteristics was further analyzed. Wound-healing, transwell migration and invasion assays tested the effect of CIP4 on cells migration and invasion ability in vitro, and the orthotopic xenograft colorectal cancer mouse mode evaluated the tumor metastasis in vivo. The invadopodia formation and function were assessed by immunofluorescence, scanning electron microscopy (SEM) and matrix degradation assay. The interaction between CIP4 and Cdc42 was confirmed by co-immunoprecipitation (co-IP) and GST-Pull down assays. Immunofluorescence was used to observed the colocalization of CIP4, GTP-Cdc42 and invadopodia. The related downstream signaling pathway was investigated by western blot and immunofluorescence.

Results

CIP4 expression was significantly higher in human colorectal cancer tissues and correlated with the CRC infiltrating depth and metastasis as well as the lower survival rate in patients. In cultured CRC cells, knockdown of CIP4 inhibited cell migration and invasion ability in vitro and the tumor metastasis in vivo, while overexpression of CIP4 confirmed the opposite situation by promoting invadopodia formation and matrix degradation ability. In addition, we identified GTP-Cdc42 as a directly interactive protein of CIP4, which was upregulated and recruited by CIP4 to participate in this process. Furthermore, activated NF-κB signaling pathway was found in CIP4 overexpression CRC cells contributing to invadopodia formation while inhibition of either CIP4 or Cdc42 led to suppression of NF-κB pathway resulted in decrease quantity of invadopodia.

Conclusion

Our findings suggested that CIP4 targets to recruit GTP-Cdc42 and directly combines with it to accelerate invadopodia formation and function by activating NF-κB signaling pathway, thus promoting CRC infiltration and metastasis.

Background

Colorectal cancer (CRC) is one of the most common tumors. In 2020, approximately 147,950 individuals are diagnosed with CRC and 53,200 died from the disease(1). Although surgical techniques and adjuvant therapy have advanced, the overall survival of CRC patients has not improved obviously in recent years(2). Liver and lung metastasis after radical resection and chemoradiotherapy is the most important cause of death in CRC patients(3). Metastasis is a complex biological process which needs cancer cells to form a leading edge and move forward(4). Invasion of cancer cells into surrounding tissue and the vasculature requires chemotactic migration of cancer cells, steered by protrusive activity of the cell membrane and its attachment to the extracellular matrix (ECM)(5). Recent work has discovered a prominent actin-based cellular structure, termed invadopodia, as unique structural and functional modules through which major invasive mechanisms are regulated(6–8). The co-localization of F-actin with actin-bundling protein cortactin combines with microtubules, driving the invadopodia to degrade extracellular matrix and to facilitate distant metastasis(9).

CIP4 (Cdc42-interacting protein 4) is a protein encoded by the TRIP10 gene located on human chromosome 19(10). CIP4 was first identified by using activated Cdc42 as a bait in a yeast two-hybrid screen which contains an F-BAR domain at the N-terminal, a SH3 domain at the C-terminal and an HR1 domain in the middle(11, 12). It has been reported that CIP4 plays an important role in various cellular events by regulating cell membranes and actin, such as vesicle formation, endocytosis, cytoplasmic membrane microtubule transformation, adhesion and invadopodia formation in a variety of cells(13–17). Other studies have associated CIP4 with cell invasiveness and migration in different types of cancer, such as breast cancer, Non-small cell lung cancer, Nasopharyngeal carcinoma, Osteosarcoma and so on, which indicates that CIP4 has a crucial part to play in tumor metastasis(18–22).

CIP4 has been identified by the interaction with the activated Cdc42. Cdc42 is a key member of the Rho family which is well established to be central to the dynamic actin cytoskeletal assembly and rearrangement, the underpinnings of normal cell–cell adhesion, cell migration, and even transformation(23). Cdc42 is also involved in the regulation of invadopodia formation(24, 25). Studies have demonstrated the podocalyxin-like 1 promotes invadopodia formation and metastasis through activation of Rac1/Cdc42/cortactin signaling in breast cancer cells(26).

NF-kB is a critical cell signaling pathway involving in many cellular activities and can result in cancer if not appropriately regulated(27). Inappropriate activation of NF-kB leads to tumor proliferation, invasion and metastasis(28, 29). Early studies showed that Cdc42 regulates specifically in the NF-kB-dependent transcription(30, 31). Therefore, in view of the special role of CIP4 and Cdc42 in invadopodia formation, along with the unknown downstream signaling pathway, whether NF-kB is in response to the activated Cdc42 interacting with CIP4 to promote CRC progression and metastasis attracted the interest of us.

Our previous research found that CIP4 expression is significantly up-regulated in human CRC tissues(32). In the current study, we demonstrated the expression and clinical significance of CIP4 in CRC samples, and provided evidences that CIP4 binds to GTP-Cdc42 to promote invadopodia formation and ECM

degradation. Importantly, we further explored the downstream regulation mechanism of the complex of CIP4 and Cdc42 in CRC progression and metastasis, in which the NF-kB signaling pathway was confirmed to be essential.

Materials And Methods

Clinical samples, cell lines and animals

Formalin-fixed paraffin embedded human colorectal carcinoma tissues (n = 107) for this study were obtained from the Department of Pathology, Nanfang Hospital, Southern Medical University, China. Each case was confirmed a definite diagnosis of primary CRC. The fresh surgically resected CRC tissues and matched adjacent normal tissues (n = 14) were immediately frozen in liquid nitrogen till the later study. Colorectal cancer cell lines, including Lovo, HT29, HCT116 and DLD1 cells were obtained from the Global Bioresource Centre (ATCC, Washington, USA). All cells were cultured in RPMI 1640 medium (Gibco, Grand Island, USA) supplemented with 10% foetal bovine serum (FBS, Gibco) at 37°C in a humidified atmosphere with 5% CO2. Four to six weeks-old male athymic BALB/c mice were purchased from the Central Laboratory of animal Science at Southern Medical University (Guangzhou, China). All animal care and experiments were approved by the Institutional Animal Care and Use Committee (IACUC) of Nanfang hospital, Southern Medical University, Guangzhou.

Reagents and antibodies

Antibody against CIP4 (Cat:612556) was purchased from BD Biosciences (NY, USA). Antibodies against GAPDH (Cat:60004), Cdc42 (Cat:10155), Cortactin (Cat:11381), Histone H3 (Cat:17168), FLAG tag (Cat:66008) were purchased from Proteintech (Illinois, USA). Antibodies against p65 (Cat:8242), p-p65 (Cat:3033), the Active Cdc42 Detection Kit (Cat: 8819) were purchased from Cell Signaling Technology (Massachusetts, USA). Antibodies against His tag (Cat:0287R) and GST tag (Cat:33007M) were purchased from Bioss (Beijing, China). The Cdc42 inhibitor ML141 and the NF-κB signaling inhibitor QNZ were purchased from Selleck Chemicals (Shanghai, China). The NF-κB signaling activator LPS was purchased from Sigma (Missouri, USA).

Western blot analysis

Total proteins from cell or tissue were separated from cells by lysis buffer (FDbio, Hangzhou, China) and the concentration was detected by BCA protein assay kits (FDbio). Proteins were separated by 10% or 12.5% SDS-PAGE gel and transferred to PVDF membranes. After being blocked by 5% skimmed milk for 1h at room temperature, the protein bands were incubated with primary antibodies at 4°C overnight. The membranes were then incubated with goat anti-mouse or anti-rabbit secondary antibody (FDbio) and detected by enhanced chemiluminescence.

Immunohistochemistry (IHC) analysis

The procedure of IHC refered to the specification of rabbit and mouse two-step immunohistochemical detection kit (ZSGB-BIO, Beijing, China). The paraffin-embedded human CRC tissue sections were incubated with primary antibodies against CIP4, Cdc42 and Ki-67 (working solution, ZSGB-BIO). Two experienced pathologists observed and scored the degree of staining in the sections independently. The staining intensity was scored as follows: 0 (no staining); 1 (light yellow); 2 (brownish yellow); and 3(brown), and the percentage of positive staining cells was scored as follow: 1 (< 10%); 2 (10%-50%); 3 (50%-70%); 4 (> 70%). Each section was comprehensively calculated by multiplication of the staining intensity score and the percentage positivity score. We defined 0 as negative, 1–4 as low, 5–8 as medium and > 8 as high.

Construction of stable cell lines

The plasmid (hU6-MCS-SV40-Neomycin) carrying CIP4-repressing shRNA sequence (shCIP4, 5'-GGAGAAUAGUAAGCGUAAATT-3') and the empty vector (shCtrl) used as control to shCIP4 were purchased from Genechem (Shanghai, China). The lentivirus vector carrying the human CIP4 sequence (CIP4) and the lentivirus containing a scrambling sequence (Ctrl) used as control to CIP4 overexpression were purchased from Genechem. The lentivirus vector carrying the FLAG-L61Cdc42 sequence, which contained a Gln61 to Leu substitution to activated Cdc42 constantly, was purchased from Genechem.

Lovo and HT29 cells were transfected with shCIP4 and shCtrl using Lipofectamine 3000 Transfection Reagent (Invitrogen, California, USA) referring to the specification. Stable cell lines were obtained by resistance screening with G418 (Sigma) at the concentration of 800μg/ml for 15 days. HCT116 and DLD1 cells were transfected with CIP4 and Ctrl, Lovo-Ctrl, Lovo-shCIP4, HT29-Ctrl, HT29-shCIP4, HCT116-Ctrl, HCT116-CIP4, DLD1-Ctrl and DLD1-CIP4 cells were transfected with FLAG-L61Cdc42 referring to the specification provided by Genechem. Stable cell lines were obtained by resistance screening with puromycin (Solarbio, Beijing, China) at the concentration of 5ng/ml for 10 days. The transfection efficiency was assessed by Western blot analysis.

Wound-healing assay

Cells ($5–10\times10^5$) were seeded into six-well plates and cultured to 90% confluence. Cell monolayers were wounded by a sterile 10μl pipette tip. The detached cells were removed by PBS. After culturing for another 48h, the wound gaps were observed and photographed by the inverted microscope (Olympus, Tokyo, Japan).

Transwell migration and invasion assays

Cells ($0.1\text{-}1\times10^6$) were resuspended in 200μL serum-free medium and seeded in the 24-well transwell upper chambers (Corning, NY, USA). 500μL RPMI-1640 medium containing 10% FBS was added into the lower chambers. After culturing for 12-48h, cells on the membrane were fixed with formalin, stained with hematoxylin and then calculated and photographed using the ordinary optics microscope (Olympus). Invasion assays were performed according to the same procedures with the diluted Matrigel (Corning) (RPMI-1640: Matrigel = 5:1) spread on the inside bottom of the transwell upper chambers.

Orthotopic xenograft colorectal cancer mouse model

The HT29-shCtrl and HT29-shCIP4 cells were prepared and suspended by fresh PBS to a concentration of 1×10^7 cells/100μl. 80μL volume of cells were injected into the scapular skin of each athymic BALB/c mice. The formed subcutaneous tumor tissues were planted separately into the cecal wall of athymic BALB/c mice. After 8 weeks, the orthotopic xenograft colorectal cancer masses and the livers of nude mice were surgically removed after euthanasia, fixed in formalin (neutral buffered 10%), embedded in paraffin, and prepared into 2.5-μm sections for hematoxylin-eosin (HE) staining and IHC analysis.

Immunofluorescence

Cells were seeded on confocal disks (Nest, Wuxi, China) and cultured for 24h, washed with PBS, fixed with 4% formaldehyde for 30 min, permeabilizated with 0.25% Triton X-100 for 8 min, blocked with goat serum (ZSGB-BIO) for 45 min and then incubated with primary antibodies at 4°C overnight. After being incubated with Alexa488/594/355 conjugated secondary antibodies (ZSGB-BIO) or rhodamine phalloidin (Cytoskeleton Inc, Colorado, USA) for 1 h and DAPI counterstaining for 10 min, the cells were observed and photographed by the Olympus confocal fluorescence microscope (FV1000).

Scanning electron microscopy (SEM)

Cells were seeded on 8mm diameter pre-cleaned coverslips and cultured in 24-well plates for 36h, then washed with PBS and fixed with 2.5% glutaraldehyde at 4°C overnight. After being washed with PBS, the cells on coverslips were dehydrated by graded ethanol at 4°C, soaked in 100% acetonum for 20 min, in 100% isoamyl acetate for 15 min and in propylene epoxide for 20 min at 45°C. The coverslips were put in vacuumed and sprayed with metal foil. Further observation was performed under the Scanning Electron Microscopy.

Matrix degradation assay

The confocal disks (Nest) were incubated with 200μl 50μg/ml polylysine, 200μl 0.5% glutaraldehyde, 200μl 0.2% gelatin from pig Oregon green 488 (Invitrogene) and 200μl 5mg/ml sodium borohydride, each for 15 min at room temperature and washed with PBS for 3 times in between. Cells (5×10^3) were seeded in each disk and cultured for 48h. The following steps were performed according to the procedures of immunofluorescence.

Co-immunoprecipitation (co-IP)

Proteins extract from Lovo cells (1×10^7) were immunoprecipitated using the primary antibodies against CIP4 or Cdc42. Input was used as the positive control and normal rabbit IgG (Cell Signaling Technology) was used as the negative control. The immu-noprecipitated proteins were then analyzed by Western blotting.

GST Pull-down

The Ctrl-GST, CIP4-GST and L61Cdc42-6HIS prokaryotic expression vectors were constructed and purchased from Genechem. The fusion proteins were induced by IPTG in BL21 (TransGene Biotech, Beijing, China) growing in LB-ampicillin. The optimum inducement condition for CIP4-GST is 0.5mM of IPTG in 16℃ for 20h, and for L61Cdc42-6HIS is 0.8mM of IPTG in 16℃ for 12h (Supplementary Fig.S2B). The proteins were purified by combining GST-agarose or His-agarose at 4°C overnight. The purified Ctrl-GST and CIP4-GST proteins were eluted from the GST-agarose and combined with L61Cdc42-6HIS fusion protein and His-agarose at 4°C overnight. After being washed for 5 times, the remaining protein mixture combined with His-agarose was analyzed by Coomassie brilliant blue staining and Western blot assays.

Statistical analysis

All statistical analyses were performed using the SPSS 24.0 (Abbott Laboratories, USA) and presented as the mean ± standard deviation. The significance of correlation between the expression of CIP4 and histopathological factors was determined using Pearson $\chi 2$ test. The enumeration data was analyzed using t-test or one-way ANOVA. Survival curves of CIP4 expression in CRC patients was carried out using the Kaplan–Meier method. P values of 0.05 or lower were considered statistically significant.

Results

1. CIP4 expression in CRC tissues correlates with tumor development, invasiveness and patient survival rate

Western blot was utilized to test the expression of CIP4 in 14 CRC tissues (T) and paired adjacent normal colorectal tissues (N). Our results revealed that CIP4 was up-regulated in all the 14 CRC tissues at the protein level ($p < 0.0001$, Fig. 1A). Immunohistochemistry (IHC) staining was performed in 107 paraffin-embedded CRC tissue sections. The representative photographs showed the expression of CIP4 was significantly elevated in human CRC tumors compared to the corresponding normal tissues. CIP4 expression score was also higher in tumor tissues ($p < 0.0001$, Fig. 1B). Interestingly, we found that CIP4 exhibit higher expression in the invasion front (a) than the tumor central area (b) in some CRC tissues (Fig. 1C). In addition, the correlation between CIP4 expression level and CRC clinicopathological characteristics was further analyzed (Table 1). we found that CIP4 level was closely related to tumor differentiation ($p < 0.001$, Table 1) and invasive depth ($p < 0.001$, Table 1).

Table 1
Clinicopathological and molecular characteristics of CIP4 expression of CRCs

Variables	No.of cases	Low	Medium	High	P-value
Age					
Younger (< = 50 years)	32(29.9%)	6(5.6%)	14(13.1%)	12(11.2%)	**0.280**
Older (> 50 years)	75(71.1%)	14(13.1%)	44(41.1%)	17(15.9%)	
Gender					
Male	70(65.4%)	12(11.2%)	38(35.5%)	20(18.7%)	**0.530**
Female	37(34.6%)	8(7.5%)	20(18.7%)	9(8.4%)	
Position					
Colon	79(73.8%)	15(14.0%)	45(42.1%)	19(17.8%)	**0.373**
Rectum	28(26.2%)	5(4.7%)	13(12.1%)	10(9.3%)	
Tumor size (maximum diameter)					
<=5cm	66(61.7%)	13(12.1%)	34(31.8%)	19(17.8%)	**0.874**
> 5cm	41(38.3%)	7(6.5%)	24(22.4%)	10(9.3%)	
Tumor grade (differentiation)					
G1	18(16.8%)	10(9.3%)	7(6.5%)	1(0.9%)	**< 0.001**
G2	82(76.6%)	10(9.3%)	50(46.7%)	22(20.6%)	
G3	7(6.5%)	0(0.0%)	1(0.9%)	6(5.6%)	
Invasive depth					
Submucosal	9(8.4%)	5(4.7%)	3(2.8%)	1(0.9%)	**< 0.001**
Myometrium	16(15.0%)	9(8.4%)	4(3.7%)	3(2.8%)	
Subserosal	82(76.6%)	6(5.6%)	51(47.7%)	25(23.4%)	
Mucinous component					
Absent	23(21.5%)	5(4.7%)	9(8.4%)	9(8.4%)	**0.437**
Present	84(78.5%)	15(14.0%)	49(45.8%)	20(18.7%)	

Moreover, to investigate whether the different levels of CIP4 expression in CRC are related to patient's prognosis, we performed bioinformatic analysis of NCBI GEO Database. Kaplan–Meier survival analysis revealed that patients with a higher level of CIP4 expression had a worse clinical outcome (P = 0.0353, Fig. 1D). These observations demonstrate that CIP4 may play an important role in CRC invasion and metastasis as well as the patient's survival.

2. CIP4 promotes CRC cells migration and invasion in vitro, and tumor metastasis in vivo

A high level of CIP4 expression was observed in Lovo and HT29 cells while HCT-116 and DLD1 showed a low level of CIP4 expression according to our previous research(32). To gain insight into the potential role of CIP4 in CRC invasion and metastasis, we generated Lovo-shCIP4, HT29-shCIP4 cell lines that stably downregulated CIP4, and HCT116-CIP4, DLD1-CIP4 cell lines that stably overexpressed CIP4 (Fig. 2A). Transwell migration assays and wound-healing assays were performed to evaluate cells migrate ability. The migration ability of Lovo-shCIP4 and HT29-shCIP4 cells were reduced compared with the control cells, while HCT116-CIP4 and DLD1-CIP4 cells showed enhanced migration ability compared with the control cells ($P < 0.05$, Fig. 2B, 2C). Matrigel-coated Boyden chamber invasion assay revealed that the knockdown of CIP4 significantly reduced the invaded cell numbers. Inversely, overexpression of CIP4 accelerated the invasion ability of HCT116-CIP4 and DLD1-CIP4 cells ($P < 0.01$, Fig. 2D).

The effect of CIP4 on tumor metastasis was assessed by an animal model for colon cancer metastasis, which spontaneously metastasizing colonic tumors were formed after suture of colon cancer tumors into the cecal wall of BALB/c-nu/nu athymic mice. 8 weeks after operation, no liver metastatic nodule was found in all five HT29-shCIP4 groups (0/5) while three out of five HT29-shCtrl groups presented liver metastatic (3/5). The numbers of nodules observed were 2, 3 and 5 respectively as shown in Fig. 2E. IHC staining confirmed that the tumors derived from HT29-shCIP4 group exhibited less CIP4 expression levels than tumors derived from control cells.

3. CIP4 is sufficient for invadopodia formation and function in CRC cells

We evaluated the effect of CIP4 on invadopodia formation by examining the co-localization of F-actin (red) with actin-bundling protein Cortactin (green) in CRC cell lines. Suppression of CIP4 reduced the occurrence of invadopodia from 45.83–19.67% in Lovo cells ($P < 0.001$, Fig. 3A) and from 26.00–16.67% in HT29 cells ($P < 0.001$, Supplementary Fig. S1A) and also shrinked the morphology of invadopodia (Supplementary Fig.S1B). Meanwhile, over 35% (HCT116,) or 38% (DLD1) of cells contained invadopodia after overexpressing CIP4, which existed as bright large puncta surrounding the nuclei, compared with 16.33% or 16.83% of control cells with smaller invadopodia respectively ($P < 0.01$, $P < 0.001$, Fig. 3A and Supplementary Fig. S1A, S1B). In addition, we observed the effect of CIP4 on the morphology of invadopodia by scanning electron microscopy (SEM). A great quantity of elongated branching invadopodia in the ventral side of Lovo were observed. The number of invadopodia reduced and the protrusions became shorter with the decreased expression of CIP4. The same phenomenon was found in HCT116 cells, the invadopodia was denser and more extended than control cells when CIP4 was overexpressed (Fig. 3B).

The matrix degradation is an indispensable step of tumor metastasis(33), so we detected the ability of invadopodia to degrade matrix gels by matrix degradation assay. Overexpression of CIP4 enlarged the cavities formed by degradation of matrix gels by approximately 2.7-fold (HCT116, $P < 0.01$), while CIP4 knockdown reduced the cavities by 2.3-fold (Lovo, $P < 0.05$) (Fig. 3C). We further observed the morphology of matrix degradation by CRC cells through scanning electron microscope. As is shown in

Fig. 3D, the cells with high levels of CIP4 expression (Lovo-shCtrl and HCT116-CIP4) inserted the invadopodia deeply into the matrix gels and disintegrate it. To the contrary, the cells with low levels of CIP4 expression (Lovo-shCIP4 and HCT116-Ctrl) appeared to be smoother and merely adhered to the surface of the matrix gels. Based on the above data, we evaluated that CIP4 is necessary and sufficient to promote invadopodia formation and focal matrix degradation in CRC cells.

4. CIP4 promotes the expression and activation of Cdc42

Cdc42 cycles between activation with GTP and inactivation with GDP(34, 35). It has been reported that overexpression of an active form of Cdc42 is sufficient to form invadosome actin cores(36). Since CIP4 was first identified as an interacting protein of Cdc42, the regulatory mechanism between them in CRC remains to be revealed. In Fig. 4A, we examined the expression levels of CIP4 in 14 pairs of colorectal cancer tissues, and we again examined the expression levels of Cdc42 in these tissues. The results showed that the protein level of Cdc42 in tumor tissue (T) was higher than that of matched normal colorectal tissue (N) as same as CIP4 ($P < 0.001$, Fig. 4A). As shown in Fig. 4B, CIP4 and Cdc42 protein expression levels in consecutive paraffin-embedded slice of human CRC tissue were detected by IHC. We confirmed that Cdc42 expression score was higher in tumor tissues (Tumor1, Tumor2) than normal tissues (Normal) ($P < 0.01$). In the meantime, we observed the consistence in the expression and localization of CIP4 and Cdc42. The bioinformatic analyses indicated that there was positive correlation between CIP4 and Cdc42 ($R = 0.297$, $P = 0.023$).

To determine if CIP4 regulates Cdc42 expression and activation, we detected the expression of Cdc42 and GTP-Cdc42 in Lovo and HT29 cells when CIP4 expression was blocked, and we found the decrease protein level of Cdc42 and GTP-Cdc42 compared with the control cells. Conversely, the raised protein level of Cdc42 and GTP-Cdc42 was found in HCT116 and DLD1 cells when CIP4 expression was increased (Fig. 4C). The immunofluorescence results also confirmed the expression of CDC42 (red) was positively correlated with CIP4 (green) (Fig. 4D).

5. CIP4 directly interacts with activated Cdc42 to accelerate invadopodia function.

Since we have demonstrated that CIP4 can promote the activation of Cdc42, whether CIP4 interacts with activated Cdc42 and participates in the process of invasion and metastasis of colorectal cancer is essential to our research. The immunofluorescence assays validated localization of CIP4 and its partial co-localization with Cdc42 (Fig. 5A). The co-localization coefficients between CIP4 and Cdc42 in Lovo cells and HT29 cells are 0.64 ($n = 5$) and 0.71 ($n = 5$), in HCT116-CIP4 and DLD1-CIP4 cells are 0.42 ($n = 5$) and 0.38 ($n = 5$) (Supplementary Fig.S2A). Moreover, Co-immunoprecipitation assay revealed that CIP4 and Cdc42 physically interacted with each other in Lovo cell (Fig. 5B).

Cdc42 has the ability to combine GDP/GTP. In response to extracellular stimuli, Cdc42 transition from an inactive GDP-bound status to an active GTP-bound status and interact with downstream effectors to propagate changes in cell behaviors [10]. We constructed a prokaryotic vector for mutant of activated Cdc42 (L61Cdc42), containing a Gln61 to Leu substitution. Next, we performed the GST-Pull down assay to see whether CIP4 combines GTP-Cdc42 directly. Coomassie brilliant blue staining showed the clear

protein bands with consistent molecular weights (GST for 26KD, CIP4-GST for 101KD and L61Cdc42-6HIS for 27KD) (Supplementary Fig.S2C). We then detected the expression of CIP4-GST and L61Cdc42-6HIS fusion protein by western blot, which showed the combination between L61Cdc42-6HIS and CIP4-GST, while the negative control GST didn't combine with L61Cdc42-6HIS. According to the results, we verified that CIP4 directly interacts with GTP-Cdc42 and might forms a complex to participate in the formation of invadopodia.

In the previous data,we have evaluated that CIP4 is necessary and sufficient to promote invadopodia formation, we then validated the localization of CIP4 (green) and its partial colocalization with Cortactin (blue) and F-actin (red) in Lovo and HT29 cells by confocal laser scanning (Fig. 5D). Representative photographs indicate that CIP4 not only promotes the formation of invadopodia, but also assemble in the invadopodia. We further constructed a lentivirus vector FLAG- L61Cdc42 that continuously activated Cdc42 mutant L61Cdc42 and transfected it into the CIP4-overexpression or CIP4-knockdown CRC cells as well as their control cells. After performing the immunofluorescence assays to locate the invadopodia (blue for Cortactin and red for F-actin) and activated Cdc42 (green for FLAG, representing the activated Cdc42), we found that in the cells with high expression level of CIP4(Lovo-shCtrl, HT29-shCtrl, HCT116-CIP4 and DLD1-CIP4), the activated Cdc42 was more likely to gather in the invadopodia, while in the cells with low expression level of CIP4 (Lovo-shCIP4, HT29-shCIP4, HCT116-Ctrl and DLD1-Ctrl), the activated Cdc42 tended to scatter throughout the cells. Therefore, we inferred that CIP4 recruits GTP-Cdc42 into the invadopodia and interacts with it, promoting the formation and function of invadopodia.

6. The NF-κB signaling pathway is involved in accelerating invadopodia formation regulated by CIP4 through GTP-Cdc42.

GTP-Cdc42 has been reported to be able to activate the NF-κB signaling pathway(31). Since NF-κB is well known to be a critical part of tumor invasion and metastasis(37, 38), we wondered if the invadopodia formation was accelerated by NF-κB, which was regulated by CIP4 through GTP-Cdc42. We investigated the effects of CIP4 on the key molecule of NF-κB signaling pathway, RelA (p65), the phosphorylation status of p65 (p-p65) and the p65 in nucleus(39, 40). As is shown in Fig. 6A and Supplementary Fig.S4A, the downregulation of CIP4 in Lovo-shCIP4 and HT29-shCIP4 cells led to the decreased expressions of Cdc42 and GTP-Cdc42 as well as p-p65 and the p65 in nucleus compared with the control cells. We then overexpressed the activated Cdc42 in Lovo-shCIP4 and HT29-shCIP4 cells, and found the expressions of p-p65 and the p65 in nucleus were reverted. After being treated with the NF-κB activator LPS(41), the expressions of p-p65 and the p65 in nucleus increased significantly while the expressions of CIP4, Cdc42 and GTP-Cdc42 remained low.

Correspondingly, the overexpression of CIP4 upregulated the expressions of Cdc42 and GTP-Cdc42 as well as p-p65 and the p65 in nucleus in HCT116-CIP4 and DLD1-CIP4 cells compared with the control cells. When treated with the Cdc42 inhibitor ML141(42), the expressions of Cdc42 and GTP-Cdc42 decreased so as p-p65 and the p65 in nucleus. After being treated with the NF-κB inhibitor QNZ(43), the expressions of p-p65 and the p65 in nucleus was suppressed while the expressions of CIP4, Cdc42 and

GTP-Cdc42 barely changed (Fig. 6B, Supplementary Fig.S4B). The optimum conditions of activator and inhibitors to treated cells were examined in Supplementary Fig.S3. These results indicated the NF-κB was the downstream pathway regulated by CIP4 through GTP-Cdc42.

Next, we detected the influence of the expression changes of these proteins on the formation of invadopodia by immunofluorescence assays (Fig. 6C-D, Supplementary Fig. S4C-D). The quantity of invadopodia was consistent with the expression level of p-p65 ($P < 0.01$), which revealed that the activation of NF-κB signaling pathway was an indispensable part of invadopodia formation. Therefore, our data demonstrated that CIP4 promotes the expression and activation of Cdc42, which activated the NF-κB signaling pathway, thereby accelerating the invadopodia formation.

Discussion

Colorectal cancer is one of the most common cancers worldwide(44). Although a large number of information on the molecular basis of CRC has been provided from numerous researches to develop all kinds of targeted therapeutic options, the clinical cure rate remains unsatisfactory(45). The main obstacle of improving the clinical treatment effect of CRC currently is metastasis, which is a complex biological process involves various molecular regulation that still needs to be clearly revealed. Therefore, to elucidate the molecular mechanism of colorectal cancer infiltration and metastasis, and to intervene and treat its progress, has important scientific significance to improve the cure rate of malignant tumors and the survival rate of patients.

In our previous study, we found significantly higher expression of CIP4 in CRC cells compared to corresponding normal tissues, and demonstrated that AKAP-9 regulates the expression of CIP4 to promote metastasis and consequently epithelial-mesenchymal transition (EMT) of CRC(32). Similar phenomenon is observed in breast cancer cells where CIP4 interacts with N-WASP in response to epidermal growth factor receptor (EGFR) increasing the formation of invadopodia and ECM degradation(19). While CIP4 is regarded as a suppressor of Src-induced invadopodia formation and invasiveness in MDA-MB-231 breast tumor cells(18). CIP4 also increases the expression and activity of matrix metalloproteinase-2 (MMP-2) by regulating EGFR signaling to promote metastasis in Non-small cell lung cancer and Nasopharyngeal carcinoma cells(20, 21). The ability of CIP4 to facilitate metastasis and invasiveness is confirmed in hepatocellular carcinoma, Osteosarcoma and renal cell carcinoma as well(22, 46, 47). Although multiple molecules signals are involved in CIP4 function on cancer cells as reported, the specific mechanism of the interaction between CIP4 and Cdc42, which is the most well-known directly related protein to CIP4, remains unclear. Therefore, we focused on exploring the association between CIP4 and Cdc42 in invadopodia formation and ECM degradation, as well as the downstream signaling pathway in response in CRC.

Our results confirmed the significant high expression of CIP4 in CRC tissues, especially in the invasion front. The functional experiments in vivo and in vitro support our assumption that CIP4 plays an important role in promoting the metastasis in CRC. Since the invadopodia formation is closely related to

CIP4, we observed the quantity and morphology as well as the ECM degradation ability changes of invadopodia in CRC cells under different expression level of CIP4, which indicates CIP4 is capable of accelerating the formation and function of invadopodia. In order to figure out whether the interaction between CIP4 and Cdc42 contributes to this cellular structure, we meticulously verified that CIP4 can upregulate the expression and activation of Cdc42 and directly combine with the activated Cdc42. We haven't been able to identify the specific binding site yet, but we conjecture it might be the HR1 domain as mentioned(48). Furthermore, we spotted an interesting phenomenon that the complex of CIP4 and GTP-Cdc42 is located on invadopodia, and GTP-Cdc42 has been proved to be recruited by CIP4 to assemble in invadopodia to maximize the impact. While further exploration of the downstream molecular mechanism is required, we noticed the wildly activated signaling pathway NF-κB in CRC, which supports tumorigenesis by enhancing cell invasion and metastasis(49, 50). As expected, the high expression level of CIP4 and activated Cdc42 results in increase phosphorylation of RelA (p65), which controlles a great extent of NF-κB activity, and promote the formation of invadopodia. On the other hand, inhibition of either CIP4 or Cdc42 leads to suppression of NF-κB pathway ended up with decrease quantity of invadopodia. These results highlight the essential role of NF-κB pathway in invadopodia formation and function regulating by interaction between CIP4 and GTP-Cdc42.

Taken together, our studies revealed the molecular mechanism of CIP4 promoting CRC infiltration and metastasis. The combination with GTP-Cdc42 and activation of NF-κB signaling pathway associated with invadopodia formation and function are first mentioned in CRC. Considering the unclarity of all the details in the interaction, along with the recent study identified the CIP4 phosphorylation by PKA on the modulation of cancer invasion(46), our further research will focus on the possible modification of CIP4 which leads to the interaction with Cdc42 as well as the specific mechanism of RelA (p65) phosphorylation regulating invadopodia formation and function.

Conclusions

In summary, we found significantly higher expression of CIP4 in CRC, which promotes the transformation of Cdc42 into the active form GTP-Cdc42 and raises its amount. CIP4 targets to recruit GTP-Cdc42 and co-locating in the invadopodia to combine with it. In the meantime, the NF-κB signaling pathway is activated by the interaction of CIP4 and GTP-Cdc42, which participates in accelerating the invadopodia formation and function, thus promoting CRC tumor invasion and metastasis (Fig. 7). Therefore, our study implicates a new treatment strategy targets on CIP4 against metastasis of CRC.

Abbreviations

CIP4
Cdc42-interacting protein 4; CRC:colorectal cancer; SEM:scanning electron microscopy; ECM:extracellular matrix; IHC:immunohistochemistry; co-IP:co-immunoprecipitation; EMT:epithelial-mesenchymal transition; EGFR:epidermal growth factor receptor; MMP-2:matrix metalloproteinase-2

Declarations

Ethics approval and consent to participate

This study was approved by the Ethics Committee of Southern Medical University, GuangZhou, China.

Consent for publication

All authors have consented to publication of the results presented in this manuscript.

Availability of data and materials

All data presented or analyzed in this study are included either in this article or in the additional files.

Competing interests

The authors have no conflicts of interest to declare.

Funding

This work was supported by National Natural Science Foundation of China (K1011482, K117280039) Provincial Science Foundation of Guangdong (G820281143) and Shenzhen Hospital of Southern Medical University.

Authors' contributions

Conceptualization, Zuguo Li and Zhiyan Hu; Methodology, Zhiyan Hu, Jiaxian Zhu and Yidan Ma; Data Curation, Jiaxian Zhu, Yidan Ma and Ting Long; Formal Analysis, Jiaxian Zhu, Yidan Ma and Ting Long; Software, Jiaxian Zhu and Lingfang Gao; Validation, Yan Zhong and Xiaoyan Wang; Writing manuscript: Jiaxian Zhu and Yidan Ma; Funding Acquisition, Zuguo Li and Zhiyan Hu; Supervision, Zuguo Li. All authors read, edited and approved the final manuscript.

Acknowledgements

We thank Xia Wang, Qingcan Sun, Xiangling Lin and Kehong Zheng for inspiring discussions and technical help. We thank the Department of Pathology, Nanfang Hospital, Southern Medical University, China for the clinical specimens.

References

1. Siegel RL, Miller KD, Goding Sauer A, Fedewa SA, Butterly LF, Anderson JC, et al. Colorectal cancer statistics, 2020. CA Cancer J Clin. 2020;70(3):145-64.
2. Eswaran J, Li DQ, Shah A, Kumar R. Molecular Pathways: Targeting P21-Activated Kinase 1 Signaling in Cancer-Opportunities, Challenges, and Limitations. Clin Cancer Res. 2012;18(14):3743-9.

3. Pretzsch E, Bosch F, Neumann J, Ganschow P, Bazhin A, Guba M, et al. Mechanisms of Metastasis in Colorectal Cancer and Metastatic Organotropism: Hematogenous versus Peritoneal Spread. J Oncol. 2019;2019:7407190.
4. Paschos KA, Majeed AW, Bird NC. Natural history of hepatic metastases from colorectal cancer–pathobiological pathways with clinical significance. World J Gastroenterol. 2014;20(14):3719-37.
5. Yamaguchi H, Wyckoff J, Condeelis J. Cell migration in tumors. Curr Opin Cell Biol. 2005;17(5):559-64.
6. Gimona M, Buccione R, Courtneidge SA, Linder S. Assembly and biological role of podosomes and invadopodia. Curr Opin Cell Biol. 2008;20(2):235-41.
7. Eddy RJ, Weidmann MD, Sharma VP, Condeelis JS. Tumor Cell Invadopodia: Invasive Protrusions that Orchestrate Metastasis. Trends Cell Biol. 2017;27(8):595-607.
8. Murphy DA, Courtneidge SA. The 'ins' and 'outs' of podosomes and invadopodia: characteristics, formation and function. Nat Rev Mol Cell Biol. 2011;12(7):413-26.
9. Bowden ET, Onikoyi E, Slack R, Myoui A, Yoneda T, Yamada KM, et al. Co-localization of cortactin and phosphotyrosine identifies active invadopodia in human breast cancer cells. Exp Cell Res. 2006;312(8):1240-53.
10. Aspenstrom P. A Cdc42 target protein with homology to the non-kinase domain of FER has a potential role in regulating the actin cytoskeleton. Curr Biol. 1997;7(7):479-87.
11. Liu S, Xiong X, Zhao X, Yang X, Wang HJJoh, oncology. F-BAR family proteins, emerging regulators for cell membrane dynamic changes-from structure to human diseases. 2015;8:47.
12. Richnau N, Fransson A, Farsad K, Aspenstrom P. RICH-1 has a BIN/Amphiphysin/Rvsp domain responsible for binding to membrane lipids and tubulation of liposomes. Biochem Bioph Res Co. 2004;320(3):1034-42.
13. Tian L, Nelson DL, Stewart DM. Cdc42-interacting protein 4 mediates binding of the Wiskott-Aldrich syndrome protein to microtubules. J Biol Chem. 2000;275(11):7854-61.
14. Saengsawang W, Taylor KL, Lumbard DC, Mitok K, Price A, Pietila L, et al. CIP4 coordinates with phospholipids and actin-associated proteins to localize to the protruding edge and produce actin ribs and veils. J Cell Sci. 2013;126(Pt 11):2411-23.
15. Saengsawang W, Mitok K, Viesselmann C, Pietila L, Lumbard DC, Corey SJ, et al. The F-BAR protein CIP4 inhibits neurite formation by producing lamellipodial protrusions. Curr Biol. 2012;22(6):494-501.
16. Roberts-Galbraith RH, Gould KL. Setting the F-BAR: functions and regulation of the F-BAR protein family. Cell Cycle. 2010;9(20):4091-7.
17. Fricke R, Gohl C, Dharmalingam E, Grevelhorster A, Zahedi B, Harden N, et al. Drosophila Cip4/Toca-1 Integrates Membrane Trafficking and Actin Dynamics through WASP and SCAR/WAVE. Current Biology. 2009;19(17):1429-37.
18. Hu J, Mukhopadhyay A, Truesdell P, Chander H, Mukhopadhyay U, Mak A, et al. Cdc42-interacting protein 4 is a Src substrate that regulates invadopodia and invasiveness of breast tumors by

promoting MT1-MMP endocytosis. 2011;124:1739-51.
19. Pichot C, Arvanitis C, Hartig S, Jensen S, Bechill J, Marzouk S, et al. Cdc42-interacting protein 4 promotes breast cancer cell invasion and formation of invadopodia through activation of N-WASp. 2010;70(21):8347-56.
20. Meng D, Xie P, Peng L, Sun R, Luo D, Chen Q, et al. CDC42-interacting protein 4 promotes metastasis of nasopharyngeal carcinoma by mediating invadopodia formation and activating EGFR signaling. 2017;36(1):21.
21. Truesdell P, Ahn J, Chander H, Meens J, Watt K, Yang X, et al. CIP4 promotes lung adenocarcinoma metastasis and is associated with poor prognosis. 2015;34(27):3527-35.
22. Koshkina N, Yang G, Kleinerman EJCcdt. Inhibition of Cdc42-interacting protein 4 (CIP4) impairs osteosarcoma tumor progression. 2013;13(1):48-56.
23. Sadok A, Marshall CJ. Rho GTPases: masters of cell migration. Small GTPases. 2014;5:e29710.
24. Nakahara H, Otani T, Sasaki T, Miura Y, Takai Y, Kogo M. Involvement of Cdc42 and Rac small G proteins in invadopodia formation of RPMI7951 cells. Genes Cells. 2003;8(12):1019-27.
25. Qadir MI, Parveen A, Ali M. Cdc42: Role in Cancer Management. Chem Biol Drug Des. 2015;86(4):432-9.
26. Lin CW, Sun MS, Liao MY, Chung CH, Chi YH, Chiou LT, et al. Podocalyxin-like 1 promotes invadopodia formation and metastasis through activation of Rac1/Cdc42/cortactin signaling in breast cancer cells. Carcinogenesis. 2014;35(11):2425-35.
27. Staudt LJCSHpib. Oncogenic activation of NF-kappaB. 2010;2(6):a000109.
28. Lu X, Yarbrough WJC, reviews gf. Negative regulation of RelA phosphorylation: emerging players and their roles in cancer. 2015;26(1):7-13.
29. Thu Y, Richmond AJC, reviews gf. NF-κB inducing kinase: a key regulator in the immune system and in cancer. 2010;21(4):213-26.
30. Hall AJBSt. Rho GTPases and the control of cell behaviour. 2005;33:891-5.
31. Perona R, Montaner S, Saniger L, Sánchez-Pérez I, Bravo R, Lacal JJG, et al. Activation of the nuclear factor-kappaB by Rho, CDC42, and Rac-1 proteins. 1997;11(4):463-75.
32. Hu Z, Liu Y, Xie L, Wang X, Yang F, Chen S, et al. AKAP-9 promotes colorectal cancer development by regulating Cdc42 interacting protein 4. 2016;1862(6):1172-81.
33. Bonnans C, Chou J, Werb Z. Remodelling the extracellular matrix in development and disease. Nat Rev Mol Cell Biol. 2014;15(12):786-801.
34. Peurois F, Peyroche G, Cherfils J. Small GTPase peripheral binding to membranes: molecular determinants and supramolecular organization. Biochem Soc Trans. 2019;47(1):13-22.
35. Reiner DJ, Lundquist EA. Small GTPases. WormBook. 2018;2018:1-65.
36. Di Martino J, Paysan L, Gest C, Lagree V, Juin A, Saltel F, et al. Cdc42 and Tks5: a minimal and universal molecular signature for functional invadosomes. Cell Adh Migr. 2014;8(3):280-92.

37. Puar YR, Shanmugam MK, Fan L, Arfuso F, Sethi G, Tergaonkar V. Evidence for the Involvement of the Master Transcription Factor NF-kappaB in Cancer Initiation and Progression. Biomedicines. 2018;6(3).
38. Vaiopoulos AG, Athanasoula K, Papavassiliou AG. NF-kappaB in colorectal cancer. J Mol Med (Berl). 2013;91(9):1029-37.
39. Viatour P, Merville MP, Bours V, Chariot A. Phosphorylation of NF-kappaB and IkappaB proteins: implications in cancer and inflammation. Trends Biochem Sci. 2005;30(1):43-52.
40. Sakurai H, Chiba H, Miyoshi H, Sugita T, Toriumi W. IkappaB kinases phosphorylate NF-kappaB p65 subunit on serine 536 in the transactivation domain. J Biol Chem. 1999;274(43):30353-6.
41. Sui H, Zhou LH, Zhang YL, Huang JP, Liu X, Ji Q, et al. Evodiamine Suppresses ABCG2 Mediated Drug Resistance by Inhibiting p50/p65 NF-kappaB Pathway in Colorectal Cancer. J Cell Biochem. 2016;117(6):1471-81.
42. Surviladze Z, Waller A, Strouse JJ, Bologa C, Ursu O, Salas V, et al. A Potent and Selective Inhibitor of Cdc42 GTPase. Probe Reports from the NIH Molecular Libraries Program. Bethesda (MD)2010.
43. Tobe M, Isobe Y, Tomizawa H, Nagasaki T, Takahashi H, Fukazawa T, et al. Discovery of quinazolines as a novel structural class of potent inhibitors of NF-kappa B activation. Bioorg Med Chem. 2003;11(3):383-91.
44. Weitz J, Koch M, Debus J, Höhler T, Galle P, Büchler MJL. Colorectal cancer. 2005;365(9454):153-65.
45. Wooster AL, Girgis LH, Brazeale H, Anderson TS, Wood LM, Lowe DB. Dendritic Cell Vaccine Therapy for Colorectal Cancer. Pharmacol Res. 2020:105374.
46. Tonucci F, Almada E, Borini-Etichetti C, Pariani A, Hidalgo F, Rico M, et al. Identification of a CIP4 PKA phosphorylation site involved in the regulation of cancer cell invasiveness and metastasis. 2019;461:65-77.
47. Tsuji E, Tsuji Y, Fujiwara T, Ogata S, Tsukamoto K, Saku K. Splicing variant of Cdc42 interacting protein-4 disrupts beta-catenin-mediated cell-cell adhesion: expression and function in renal cell carcinoma. Biochem Biophys Res Commun. 2006;339(4):1083-8.
48. Kobashigawa Y, Kumeta H, Kanoh D, Inagaki FJJobN. The NMR structure of the TC10- and Cdc42-interacting domain of CIP4. 2009;44(2):113-8.
49. Naugler WE, Karin M. NF-kappaB and cancer-identifying targets and mechanisms. Curr Opin Genet Dev. 2008;18(1):19-26.
50. Patel M, Horgan PG, McMillan DC, Edwards J. NF-kappaB pathways in the development and progression of colorectal cancer. Transl Res. 2018;197:43-56.

Figures

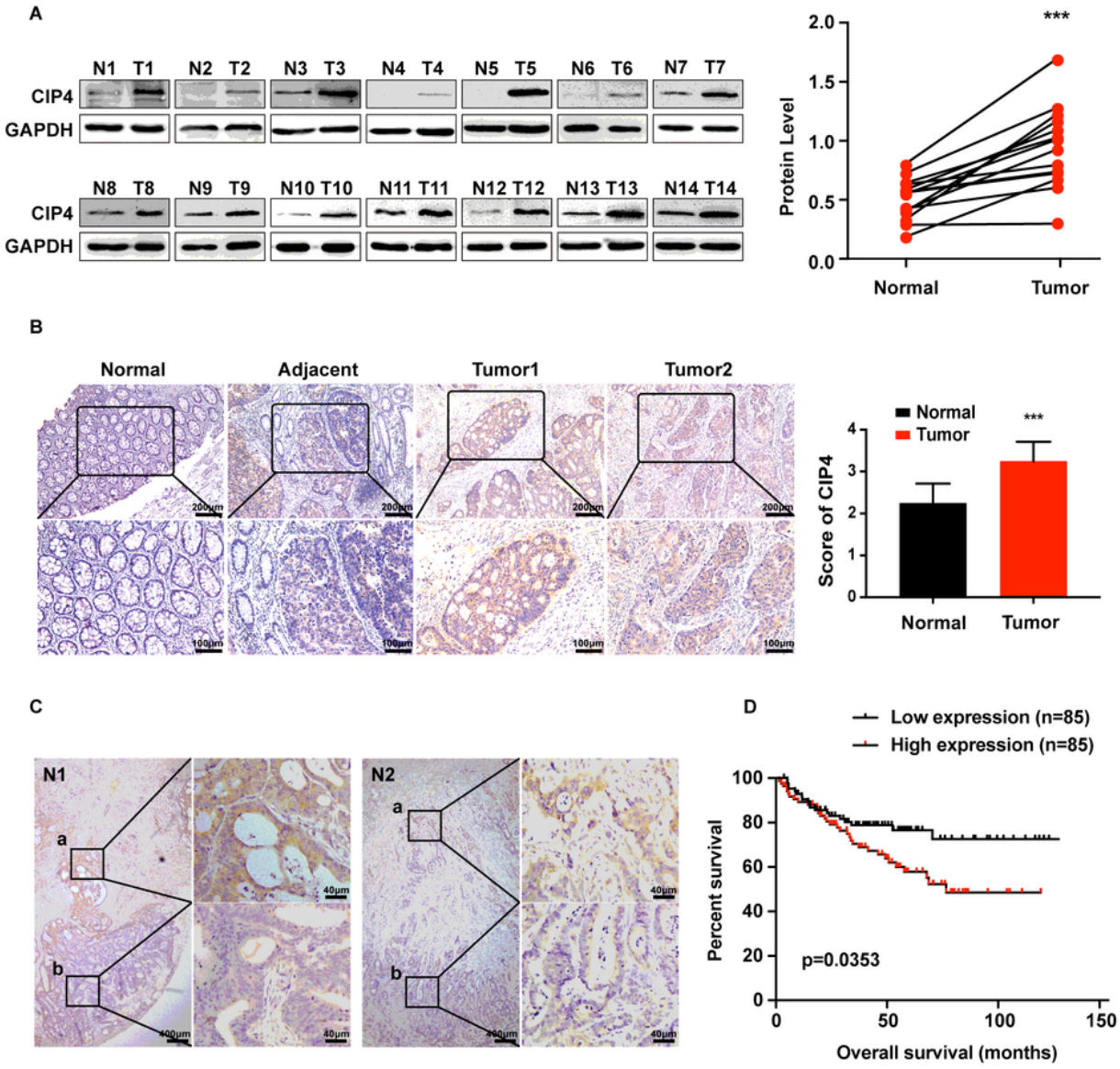

Figure 1

CIP4 expression in CRC tissues correlates with tumor development, invasiveness and patient survival rate. (A) CIP4 protein expression in fourteen pair of human CRC tissues (T) and adjacent normal tissues (N) was detected by Western blot. Quantification of protein levels were normalized to GAPDH. ***P<0.0001. (B) CIP4 protein expression in 107 paraffin-embedded normal human colorectal tissue (normal) and CRC tissues (adjacent, Tumor1, Tumor2) was detected by immunohistochemical staining (scale=200μm,

100μm) and analyzed by scores. ***P<0.0001. (C) Comparison of CIP4 expression in the invasion front (a) and tumor central area (b) of colorectal cancer. (D) Bioinformatics analysis shows the relationship between CIP4 expression and patient survival times. P=0.0353.

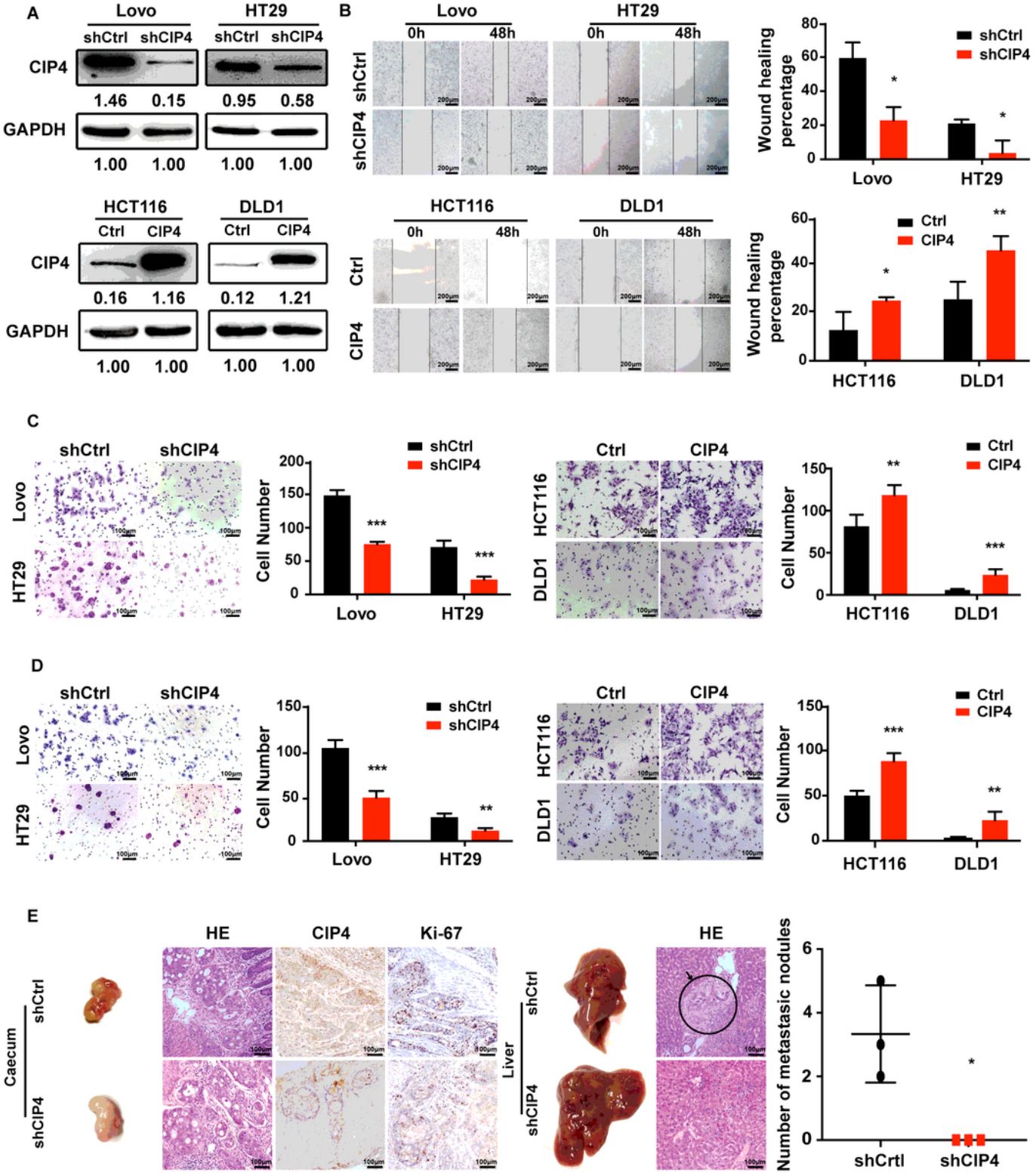

Figure 2

CIP4 promotes CRC cells migration and invasion in vitro, and tumor metastasis in vivo. (A)The establishment of CIP4 stable knockdown (Lovo and HT29) and overexpression (HCT116 and DLD1) cell

lines. CIP4 protein expression was detected by western blotting. (B) Wound healing assay was performed to evaluate cells migrate ability (scale=200μm), and cells migrate ability was identified by wound healing percentage. Error bars represent the mean ± S.D (n=5). *P<0.05, **P<0.01. (C) The cell migrate ability in CRC cells was detected by transwell migration assay (scale=100μm). Error bars represent the mean ± S.D. **P<0.01, ***P<0.001. (D) The invasion ability in CRC cells was detected by Matrigel-coated Boyden chamber invasion assay (scale=100μm). Error bars represent the mean ± S.D. **P<0.01, ***P<0.001. (E) The effect of CIP4 on tumor metastasis was assessed by an orthotopic xenograft colorectal cancer mouse model. The number of liver metastatic nodules in individual mice was counted under the microscope and analyzed (*P<0.05, n=3).

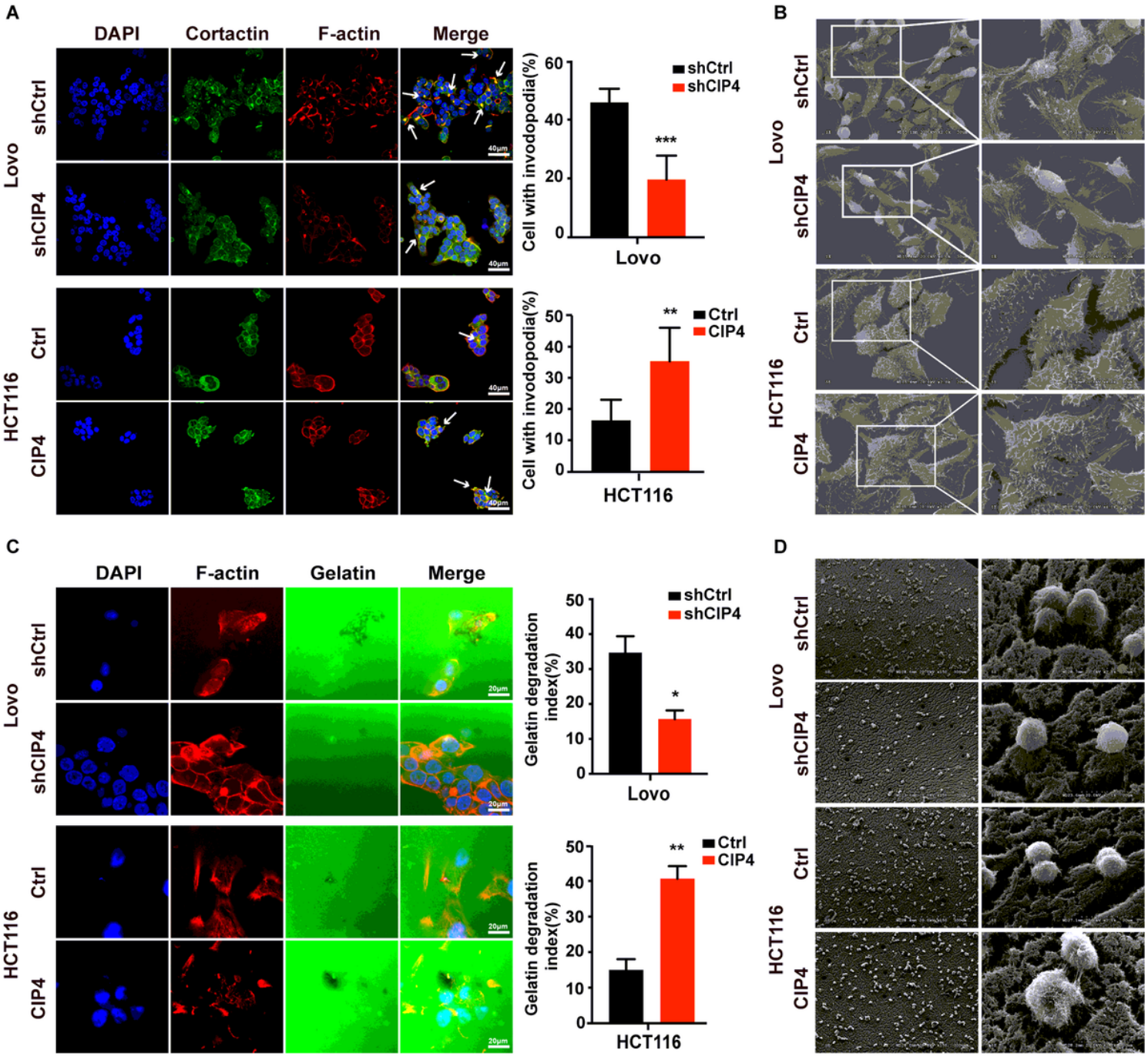

Figure 3

CIP4 is sufficient for invadopodia formation and function in CRC cells. (A) Quantification of cells with invadopodia was analyzed by immunofluorescence. White arrowhead indicates the invadopodia. Error bars represent the mean ± S.D (n=200 cells). **P<0.01, ***P<0.001. Magnification: 60x. (B) Scanning Electron Microscopy (SEM) showed the cell morphology in indicated cells. Magnification: 1000x, 2000x. (C) Matrix degradation assay was performed to analyze the invasion ability in cells. The quantification of FITC-gelatin degradation was detected by immunofluorescence. Error bars represent the mean ± S.D (n=100 cells). *P<0.05, **P<0.01. Magnification: 120x. (D) SEM showed the morphology of Matrix degradation. Magnification: 150x, 2000x.

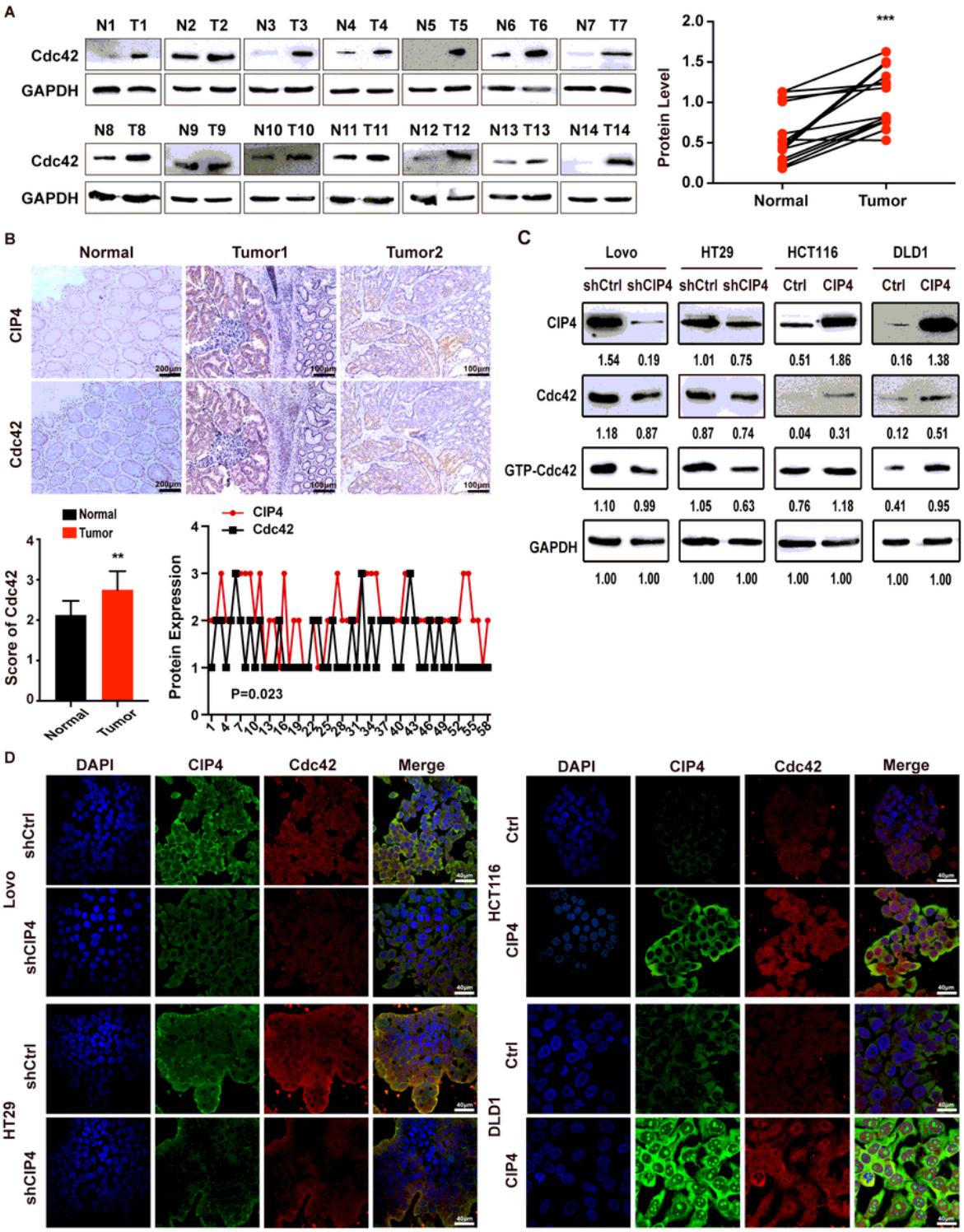

Figure 4

CIP4 promotes the expression and activation of Cdc42. (A) Cdc42 protein expression in fourteen pair of human CRC tissues (T) and adjacent normal tissues (N) was detected by Western blot. Quantification of protein levels were normalized to GAPDH. ***P<0.001. (B) Cdc42 expression was detected by immunohistochemistry staining in 58 paraffin-embedded normal human colorectal tissues and CRC tissues and analyzed by scores. **P<0.01. Representative photographs of CIP4 and Cdc42 IHC staining

(scale=200μm, 100μm) of normal tissue (Normal) and CRC tissue (Tumor 1, Tumor 2) as indicated. Spearman's correlation analysis showed the relationship between the CIP4 and Cdc42 expression levels in 58 human CRC tissues (r=0.297, P=0.023). (C) Western blot analyzed the expression of CIP4, Cdc42 and GTP-Cdc42 in CIP4 knockdown Lovo and HT29 cells and CIP4 over-expressing HCT116 and DLD1 cells. Grayscale values were normalized to GAPDH. (D) The expression of CIP4 and Cdc42 in indicated cells was observed by immunofluorescence. Magnification: 60x.

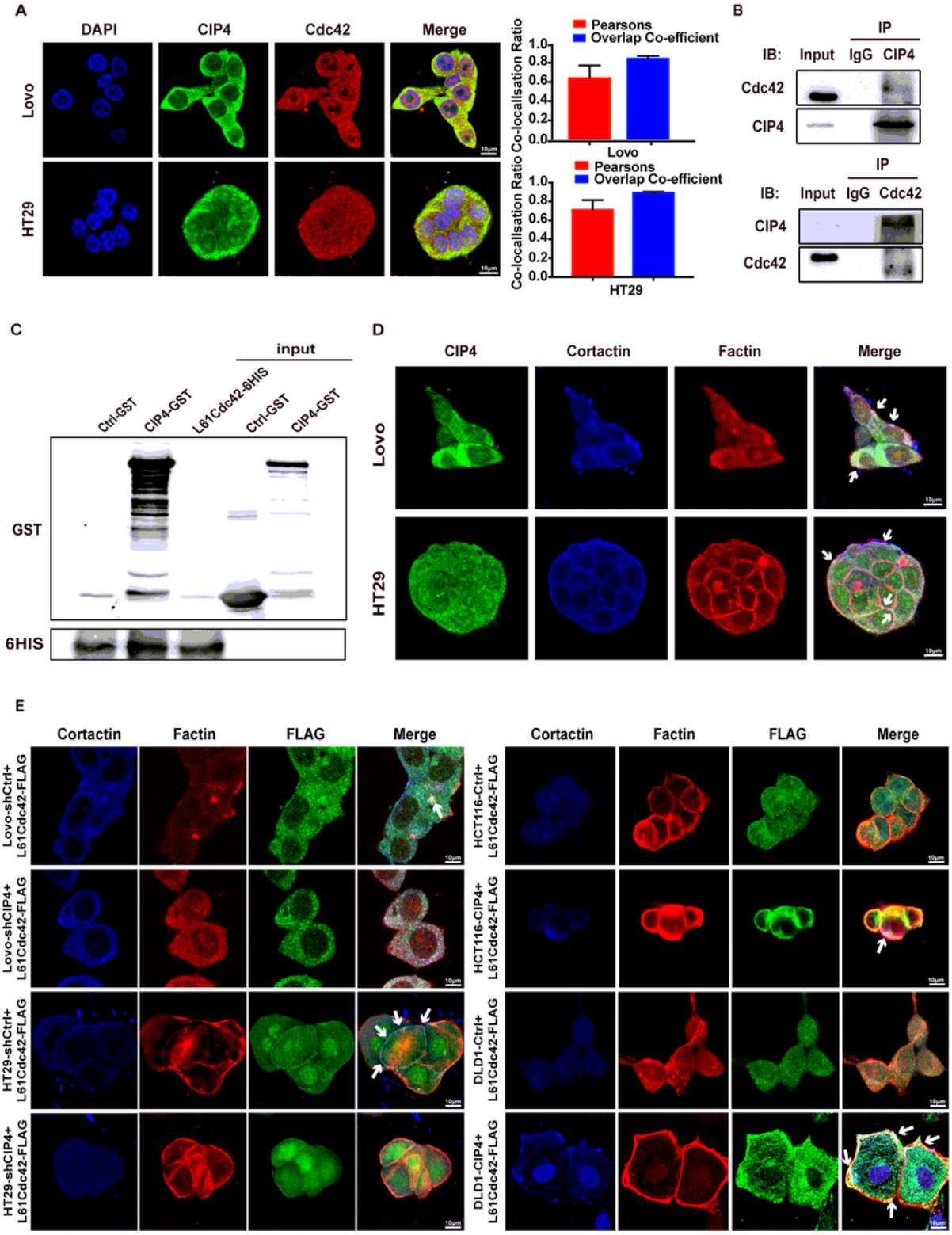

Figure 5

CIP4 directly interacts with activated Cdc42 to accelerate invadopodia function. (A) Co-localization of CIP4 (green) and Cdc42 (red) in Lovo and HT29 cells was observed by immunofluorescence. Magnification: 180x. The Person's correlation and overlap coefficient were shown in bar graph format. Error bars represent the mean±S.D (n=5). (B) Coimmunoprecipitations were performed to validate the interaction between CIP4 and Cdc42 in Lovo cells. (C) GST-Pull down experiment of CIP4 protein with mutant of activated Cdc42. GST and His were analyzed by Western blot. (D) The localization of CIP4 and invadopdia was observed in Lovo and HT29 cells by confocal laser scanning. White arrowhead indicates the co-localization of CIP4 and invadopodia. Magnification: 180x. (E) The localization of flag-tagged activated Cdc42 and invadopdia was observed in CIP4 over-expression or low-expression cells by confocal laser scanning. White arrowhead indicates the co-localization of flag-tagged activated Cdc42 and invadopodia. Magnification: 180x.

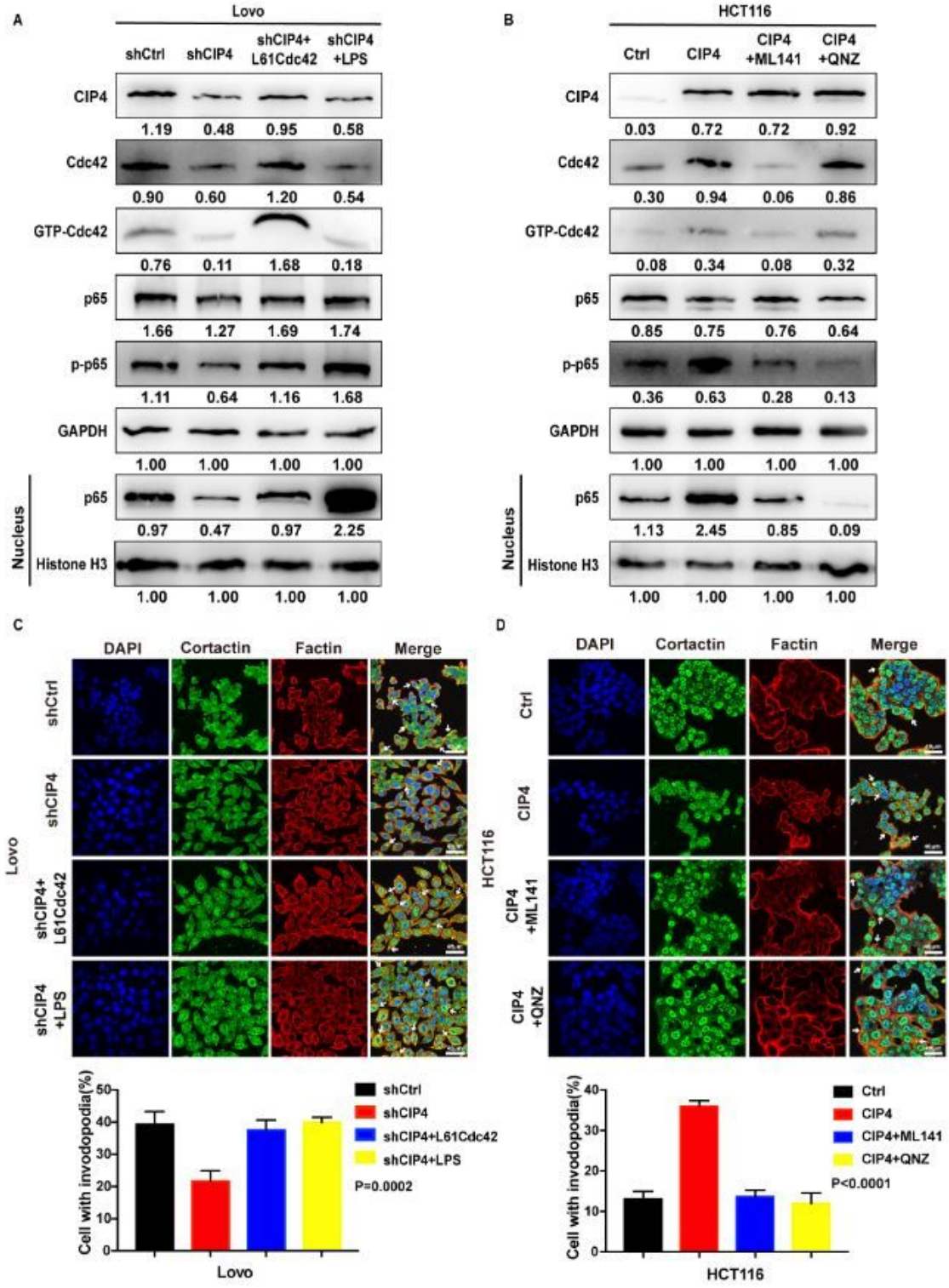

Figure 6

The NF-κB signaling pathway is involved in accelerating invadopodia formation regulated by CIP4 through GTP-Cdc42. (A-B) western blot analyzed the expression of CIP4, Cdc42, GTP-Cdc42, p65, p-p65 and p65 in nucleus in Lovo (the CIP4-knockdown cells were treated with LPS, 10 μg/ml for 0.5h) and HCT116 (the CIP4-overexpression cells were treated with ML141, 20μM for 36h, or QNZ, 10μM for 8h) cells as indicated. Grayscale values were normalized to GAPDH and histone H3 in the nucleus. (C-D)

Quantification of cells with invadopodia was analyzed by immunofluorescence. Lovo CIP4-knockdown cells were treated with LPS, 10 µg/ml for 0.5h, HCT116 CIP4-overexpression cells were treated with ML141, 20µM for 36h, or QNZ, 10µM for 8h. White arrowhead indicates the invadopodia. Error bars represent the mean ± S.D (Lovo: P=0.0002, HCT116: P<0.0001, n=200 cells). Magnification: 60x.

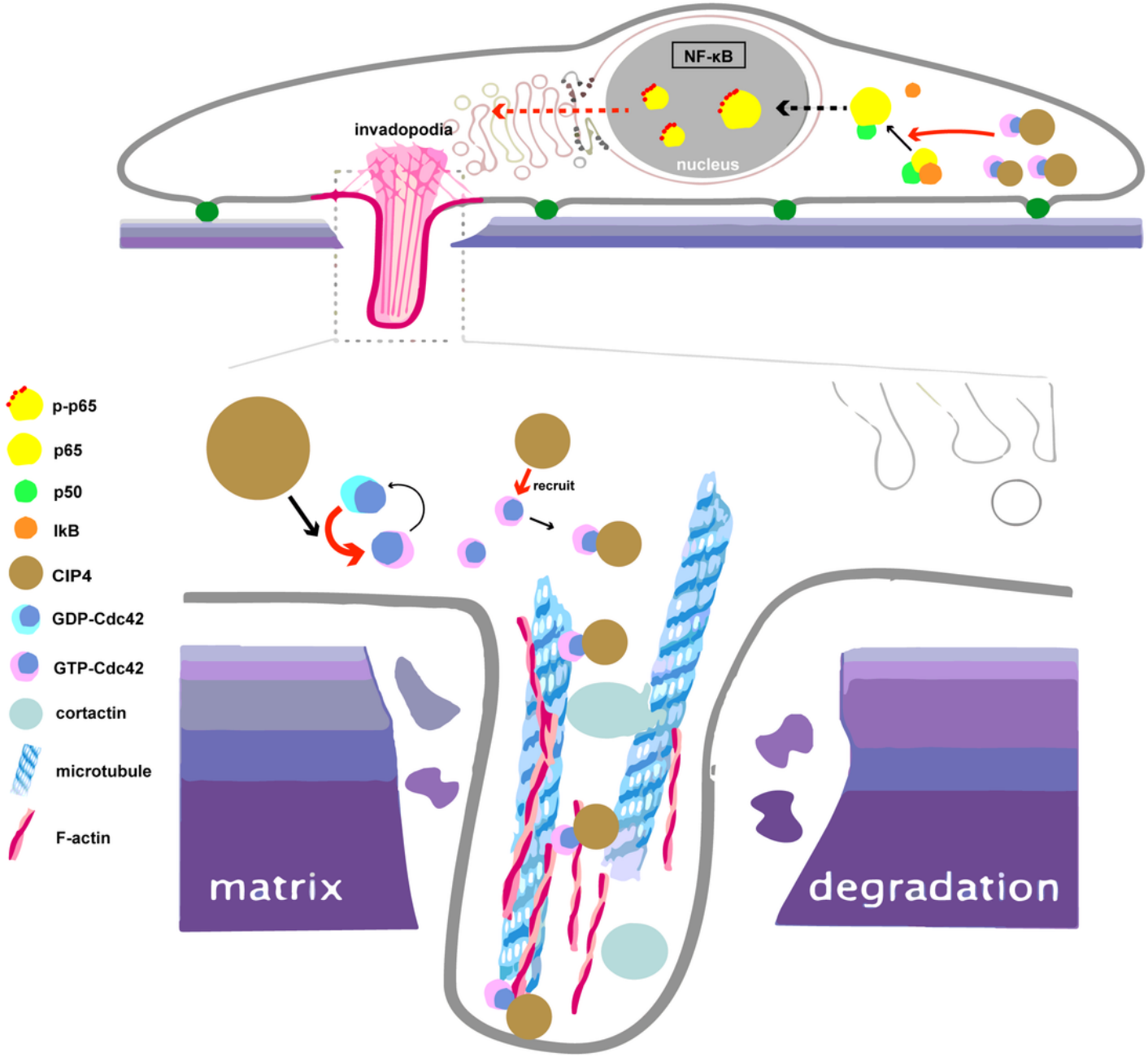

Figure 7

The schematic of the molecular mechanism of CIP4 accelerating invadopodia formation in colorectal cancer. In colorectal cancer cells, Cdc42 circulates between inactive (GDP-Cdc42) and active (GTP-Cdc42) forms. CIP4 promotes the transformation of Cdc42 into the active form, and raises the amount of GTP-Cdc42. By interacting with GTP-Cdc42, CIP4 targets to recruit GTP-Cdc42 and co-locates in the invadopodia. In the meantime, the NF-κB signaling pathway is activated by the increase of the CIP4 and GTP-Cdc42 complex, which participates in accelerating the invadopodia formation and function, thus promoting tumor invasion and metastasis.

Supplementary Files

This is a list of supplementary files associated with this preprint. Click to download.

- Additionalfile1.tif
- Additionalfile2.tif
- Additionalfile3.tif
- Additionalfile4.tif